Plasma-wall interactions during silicon etching processes in high-density HBr/Cl2/O2 plasmas

Gilles Cunge, Martin Kogelschatz, Olivier Joubert, N. Sadeghi

Plasma–wall interactions during silicon etching processes in high-density $HBr/Cl_2/O_2$ plasmas

G Cunge[1], M Kogelschatz[2], O Joubert[1] and N Sadeghi[2]

1 Laboratoire des Technologies de la Microélectronique, CNRS, 17 rue des Martyrs (CEA-LETI) 38054 Grenoble Cedex 9, France
2 Laboratoire de Spectrométrie Physique (UMR 5588), Université Joseph Fourier-Grenoble, & CNRS, BP 87, 38402 St Martin d'H`eres, France

Abstract
We have investigated the production and loss kinetics of SiClX radicals during silicon gate etching processes in HBr/Cl2/O2 plasmas. The absolute concentrations of SiClX (X = 0–2) radicals have been measured by broad band UV absorption spectroscopy at different O2 gas flow rates in the process gas mixture, and at different RF powers injected in the plasma. At the same time, the chemical composition of the layer deposited on the reactor walls has been investigated by x-ray photoelectron spectroscopy analysis. Without O2 in the plasma, the reactor walls stay clean because the silicon containing compounds redeposited on them (from Si, SiCl, Si+ and SiCl+ precursors) are subsequently etched by Cl atoms and recycled back into the plasma as SiCl2 and SiCl4 volatile species. Hence, the reactor walls are a region of production for these species, leading to their high concentrations in the gas phase. The introduction of O2 gas into the plasma results in the oxidation of the silicon chloride radicals resident on the surfaces and in the appearance of a silicon oxychloride layer on the reactor walls, whose deposition rate increases rapidly with the O2 flow. As a consequence, the production rate of SiCl2 by the reactor walls decreases because a part of the silicon containing species redeposited on the reactor walls is oxidized and incorporated in the silicon oxychloride film instead of being recycled back into the plasma as SiCl2 and SiCl4. Finally, a simple zero-dimensional model is built to predict the densities of SiClX radicals from the measured densities of SiClX+1 radicals and SiCl+ X ions. The comparison between the calculated and measured densities at different RF powers allowed us to conclude that SiCl and Si radicals are produced both in the gas phase by electron impact dissociation of SiCl2 (SiCl) radicals, and at the reactor walls by the neutralization and reflection of approximately 50% of the SiCl+ (Si+) ions impinging on these surfaces. At the same time, SiCl and Si are estimated to be lost (adsorption and abstraction reactions) on the reactor walls with a probability ranging between 0.2 and 1.

1. Introduction

Plasma etching has been successfully used in the past 20 years for fine-pattern transfer in the active parts of ultra-large-scale integrated (ULSI) circuits [1]. However, as the semiconductor industry continues to scale down the dimensions of ULSI circuits below 60 nm, a more and more precise control of the line shape profile of the etched features is required [2]. In silicon gate etching, presently done with HBr/Cl_2 based plasmas, the process must be highly anisotropic since the final dimensions of the gate must be controlled within a few nanometres only. Such a precise control of the shape of

the features requires a detailed knowledge of various etching (or deposition) mechanisms involved in the process. For example, anisotropic etching of silicon relies on the deposition of a thin passivation layer on the gate sidewalls [3]. The silicon oxychloride passivation layer is formed from the redeposition, followed by oxidation of $SiCl_X$ and/or $SiBr_X$ etch products on the gate sidewalls, and the thickness of this layer controls the final shape of the gates [4, 5]. Therefore, the redeposition of silicon etching by-products on the gate sidewalls plays a major role in the mask transfer processes.

Another important parameter of silicon etching processes in Cl_2 (or HBr) and O_2 plasmas is the deposition of a similar silicon oxychloride layer on the plasma chamber walls [6–8]. The formation of this layer on the Al_2O_3 chamber walls of industrial reactor chambers changes the surface recombination rates of the reactive species of the plasma (Cl, Br, O, H, $SiCl_X$, ...), which, in turn, modifies their gas phase concentrations [7–9], leading to a large and uncontrolled shift in the etching process. These process drifts associated with changes of the reactor wall conditions are a major issue in silicon etching processes, and it is thus important to understand the deposition mechanism of the $SiOCl_X$ layer on the reactor walls. In particular, it is necessary to analyse the production and loss kinetics of silicon etch products ($SiCl_X$ radicals), some of which are the precursors to the formation of a silicon oxychloride film on all surfaces exposed to the plasma. This is particularly important for the development of accurate feature profile evolution models, which are used to estimate the influence of the external plasma parameters on the etching characteristics, allowing faster development of etching recipes and reactor design [10]. While considerable modelling effort has been made in the past ten years for the silicon–chlorine system in high density plasmas, these models still rely on the knowledge of $SiCl_X$ radicals fluxes to the surface and their respective sticking coefficients. But the surface reactivity of $SiCl_X$ radicals and ions has never been measured, while the chemical composition of the layers deposited on the reactor walls during silicon etching processes has only been studied recently [6, 11]. This information is essential to improve the reproducibility of gate etching processes and to improve numerical models of Cl_2-based plasmas.

So far, it has been clearly shown by *ex-situ* measurements [12], by *in-situ* multiple total internal reflection Fourier transform infrared spectroscopy (MTR-FTIR) [13] and by quasi *in-situ* x-ray photoelectron spectroscopy (XPS) analyses [6], that the reactor walls stay clean when silicon is etched in a Cl_2-based plasma *without* O_2, and that a silicon oxychloride layer is deposited on the reactor walls during silicon etching in Cl_2/O_2 mixtures. However, the deposition mechanisms of these layers and in particular the nature of the silicon containing precursors that redeposit on the surface remains unclear. Ullal *et al* [13] have suggested that $SiCl_X$ radicals can only stick on O sites at the surface, explaining why there was no deposition observed without O_2. By contrast, Cunge *et al* [14] and Joubert *et al* [6] have suggested that $SiCl_X$ ($X < 2$) radicals always redeposit on the reactor walls (even without O sites) where they can either be etched by Cl atoms and recycled into the plasma as $SiCl_2$ and $SiCl_4$, or oxidized by O atoms and incorporated in the film [14]. In this scheme, there is no silicon accumulation on the reactor walls without O_2 because the layer deposited on the surfaces exposed to the plasma is removed by Cl atoms if it has not been oxidized by O atoms. This conclusion is in good agreement with the assumptions made by Lee *et al* [15] in their model. This deposition mechanism is also supported by our previously reported work [16]: a Cl-rich silicon oxychloride layer can be fully oxidized when exposed to an Ar/O_2 plasma, demonstrating that Si–Cl bonds in the bulk of the film can be oxidized by O atoms. Furthermore, Kogelschatz *et al* [16] have shown that the top surface of the silicon oxychloride layer is Cl-rich, while deeper down it is more oxidized. These density gradients are observed because oxygen atoms penetrate the film as it grows, such that the part of the film that forms first will have the greatest opportunity to be oxidized. Thus, the extent of oxidation will increase from the surface into the film.

Cunge *et al* [17] have found that in HBr/Cl_2 plasmas under similar conditions large fluxes of $SiCl^+$ and Si^+ ions are impinging on the reactor walls. These ions are also potential precursors for silicon deposition on the reactor walls and Sakai *et al* [18] have shown that the deposition yield of low energy $SiCl^+$ ions on silicon is high (about 0.6), and that the deposition mechanism may also result in $SiCl_2$ production from the surface.

All the observations mentioned above suggest that in oxygen poor conditions the reactor walls produce volatile $SiCl_2$ and $SiCl_4$ molecules and consume Si and SiCl radicals and Si^+ and $SiCl^+$ ions.

In low pressure plasmas, the surface reactivity of radicals with the surfaces exposed to the plasma controls, to a large extent, their gas phase density. Hence, the measurement of the $SiCl_X$ radical densities during silicon etching can provide information on the production and loss mechanisms of these radicals. For example, Lee *et al* [15] have shown that for non-reactive reactor walls (zero sticking coefficient for all radicals and ions), atomic silicon should be the predominant etch product in the plasma. In contrast, in the case of reactive walls (where Si, SiCl and ions can stick, and where $SiCl_2$ and $SiCl_4$ can be produced), $SiCl_2$ would be the predominant etch product in the plasma volume.

In this paper, we have used broad band UV absorption spectroscopy to measure the absolute concentration of $SiCl_X$ ($X = 0$–2) radicals and mass spectrometry to monitor the ion flux to the walls with different O_2 gas flows and RF inductive powers during silicon gate etching processes in $HBr/Cl_2/O_2$ plasmas. In parallel, when studying the influence of the O_2 flow rate, the chemical nature and deposition rate of the silicon oxychloride layer on the reactor walls have been measured in another reactor by *in-situ* XPS under the same conditions, and the silicon etch rate has been measured by reflectometry. This allows us to discuss the production and loss mechanisms of $SiCl_X$ radicals and $SiCl_X^+$ ions in the plasma and at surfaces exposed to the plasma.

2. Experimental set-up

The experimental set-up was extensively described in our recent papers [16, 19, 20]. Briefly, absorption experiments are carried out in an industrial inductively coupled plasma (ICP) source (LAM 9400) while etching 200 mm diameter blanket silicon wafers (figure 1). In all the experiments described

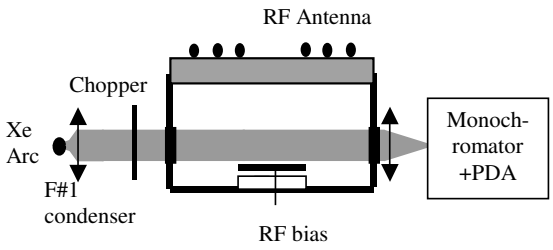

Figure 1. Experimental set-up for UV absorption measurements.

below, the wafer temperature is kept at 65°C by helium cooling of the back (electrostatic chuck), while the anodized aluminium walls of the chamber are kept at 60°C. The plasma is excited by feeding an antenna (lying on a quartz roof) with 13.56 MHz RF power, while the energy of the ions bombarding the wafer is independently controlled by a second 13.56 MHz RF power supply. Typical gate etching process plasmas operating in a HBr (120 sccm)/Cl_2 (60 sccm)/O_2 (5 sccm) gas mixture at 5 mTorr with 300 W RF inductive power and 90 W RF bias power have been used. In this process, the gas residence time is about 35 ms (the reactor body is considered to be a cylinder 38 cm in diameter and 14 cm in height, having a volume of about 16 litres). The silicon wafer etch rate is measured by *in-situ* reflectometry at 630 nm. The reactor walls are conditioned for 1 min with the etching plasma of interest prior to the UV absorption experiments for the species density measurements. The plasma chamber is then cleaned to restore Al_2O_3 reactor walls with a SF_6/O_2 plasma prior to the next experiment.

A 150 W UV-enhanced Xe arc lamp (Oriel) served as a continuum source. The optical path of the 1 cm diameter beam is located just above the wafer. The UV beam crosses the chamber through two sapphire windows that are separated from the plasma by two 10 cm long tubes, 1.5 cm in diameter, whose role is to prevent deposition on and etching of the windows. A 50 cm focal length monochromator equipped with either a 2400 grooves mm^{-1} holographic grating or a 1200 grooves mm^{-1} ruled grating blazed at 300 nm disperses the UV light, which is then detected by a 1024-channel photodiode array (Oriel Instaspec II PDA). The details of UV absorption measurements [21], the absorption spectra of $SiCl_X$ ($X = 0$–2) radicals, and the way to deduce the absolute concentrations of these species have been presented in detail in a recent paper [20]. With a few seconds acquisition time, absorbance features of 10^{-4} could be measured with a good signal to noise ratio.

The Si atom density in all low-lying long-lived states, i.e. the three sublevels of the triplet ground state: $^3P_0$, $^3P_1$, $^3P_2$ and two singlet metastable states $^1D_2$ and $^1S_0$ [22] has been determined from the measured absorbance on five transitions (251.43 nm, 250.69 nm, 252.85 nm, 288.16 nm and 263.1 nm, respectively [23]) ending in these levels [20]. For the determination of the absolute density of SiCl and $SiCl_2$ radicals, we have used absorption on the $B\,^2\Sigma^+$–$X\,^2\Pi$ transition around 290 nm [24] and the $\tilde{A}\,^1B_1$–$\tilde{X}\,^1A_1$ transition near 320 nm [25], respectively. For each species, the uncertainty in the relative densities resulting from the determination of the absorption rates (including uncertainty in the baseline and the shot noise) is about 15%. However, determination of the absolute densities also requires a knowledge of the transition probabilities. While the uncertainty in this latter value is about 5% for Si [26, 27] and $SiCl_2$ [25], it is estimated to be about 10–15% for SiCl [28]. Consequently, the estimated uncertainties in the absolute densities are about 20% for Si and $SiCl_2$ and 30% for SiCl.

During the process, the gas temperature has been deduced from the linewidth of the measured Doppler absorption profile of the 811.53 nm line ($1s_5 \rightarrow 2p_9$ transition) absorbing from Ar^* ($^3P_2$) metastable atoms. To do that, 10% of Ar was added to the $HBr/Cl_2/O_2$ plasma to generate Ar^* metastable atoms in the discharge. It has been shown that the translational temperature of these atoms is in equilibrium with the background gas [29]. The 811.53 nm beam from an external cavity tunable diode laser (Toptica DL 100) is attenuated (to avoid saturation of the absorption [30]) and split into two parts. The first part of the beam goes through a reference argon discharge cell in which Ar^* metastable atoms are created at room temperature by a weak dc discharge (1 mA) in pure Ar at 1 Torr, while the second part of the beam passes through the reactor. The laser wavelength is slowly (10 Hz) scanned around the absorption wavelength (811.53 nm) by modulating the diode laser current [31]. The intensities of the laser beams transmitted through these two plasmas are detected with two photodiodes and recorded simultaneously with a digital oscilloscope interfaced to a PC. To improve the signal to noise ratio, signals are averaged over 256 laser frequency scans before being stored in the PC. For each plasma condition, signals with (I) and without (I_0) discharges are saved for both the reference cell and the process plasma. The gas temperature T in each plasma is related to the width (FWHM) of the curve $\ln(I/I_0)$ versus wavelength [31]: $\gamma\,(\mathrm{FWHM}) = (2\sqrt{\ln 2}/\lambda_0)\sqrt{k_B T/M}$. As the frequency scan of the laser diode is almost linear with the modulation current, the translational temperature of argon metastable atoms in the process plasma, T_{pp}, is given by $T_{pp} = 300 \times (\gamma_{pp}/\gamma_{rd})^2$, where γ_{pp} and γ_{rd} are the widths (FWHM) of the $\ln(I/I_0)$ profiles of the process plasma and reference argon discharge and 300 accounts for the gas temperature in the reference discharge. In the Torr range, low current plasmas, metastable atoms are produced by electron impact excitation of ground state atoms and due to metastability exchange collisions, they are in complete kinetic equilibrium with argon atoms [29], which are at room temperature. In the low pressure process plasma, metastable atoms are produced by electron impact excitation and are mainly quenched by collision with reactive halogen containing species, for which the quenching rate coefficients are very large [32]. Therefore, their lifetime in the plasma is short and their kinetic energy reflects the kinetic energy of the ground state atoms that are in thermodynamic equilibrium with the neutral species of the process plasma.

As an example, figure 2 shows the absorption line profile from the reference discharge cell and from the process reactor with a 450 W source power $HBr/Cl_2/O_2/Ar$ (120/60/5/10 sccm) plasma at 5 mTorr. The gas temperature in the process plasma deduced from these profiles is $T_g = 485 \pm 40$ K. We should point out that the amplitude of the absorption signal is about one order of magnitude larger for the reference cell than for the process plasma, whereas the corresponding

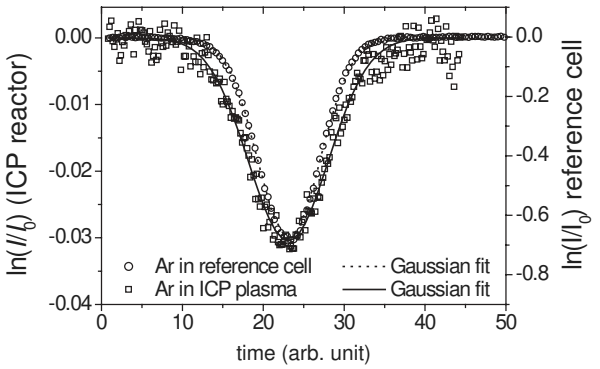

Figure 2. Doppler broadened 811.5 nm absorption line profiles on Ar^* metastables recorded with the diode laser: (○) from the reference discharge cell (dc discharge, 300 K) and (□) recorded in the $HBr/Cl_2/O_2/Ar$ plasma (120/60/5/10 sccm) at 5 mTorr total pressure and 450 W RF source power.

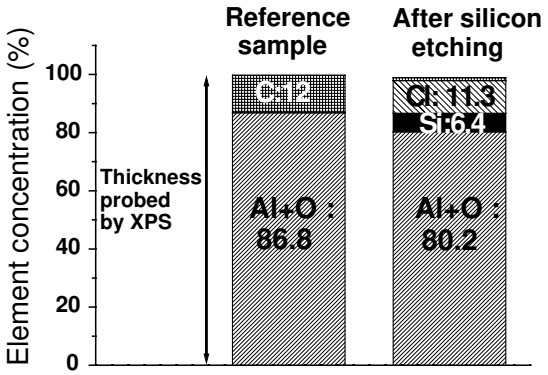

Figure 3. XPS analysis of the Al_2O_3 sample that simulates the reactor walls. Left figure: reference before exposure to the plasma; right figure: after the sample exposure to the silicon etching plasma for 80 s (plasma conditions: HBr/Cl_2 (120 : 60 sccm), 5 mTorr, 450 W RF source power (equivalent to 300 W in the LAM reactor) and 90 W RF bias power). The thickness probed by XPS is typically about 10–15 nm.

absorption path lengths are 2 cm and 40 cm, respectively. The density of metastable atoms in the process plasma is almost three orders of magnitude smaller compared to the low current argon discharge. This is a direct consequence of the quenching of these atoms by the process gas. As an example, the rate coefficients for quenching by Cl_2 and HBr are 71×10^{-11} cm^3 s^{-1} and 52×10^{-11} cm^3 s^{-1}, respectively [32].

From the absorption profiles recorded at different plasma conditions, we can conclude that the gas temperature in the $HBr/Cl_2/O_2$ plasma is about 480 ± 40 K for RF source power between 150 and 600 W.

Quantitative ion fluxes and ion mass spectra have been measured [17] by a planar capacitively coupled ion flux probe [33] and by a mass spectrometer, respectively, at the chamber wall position of another ICP reactor (DPS from Applied Materials Inc.). These measurements have been described in detail elsewhere [17]. Since the chamber volumes of the two reactors are different, the RF power of [17] has been divided by a factor of $\frac{3}{2}$ to adjust the power density (W cm^{-3}) injected into the plasma used in this work for the same gas mixture (450 W in the 25 litres volume of the DPS inductively coupled reactor of [17] is approximately equivalent to 300 W in the 16 litres volume of the present LAM 9400 reactor). It has been checked that at constant RF power density, both reactors provide approximately the same silicon etch rate and gate etching profiles, so that the results obtained in both reactors can be compared.

Finally, in recent papers [6, 34] we have presented a new technique, which allows us to measure by XPS the chemical nature and thickness of the layers deposited on the reactor walls during an etching process. These layers are deposited on a floating Al_2O_3 sample, which is fixed on the silicon wafer, but separated from it by a 3 mm thick air gap. The air gap is created by making four small cylindrical rolls (3 mm diameter each) with adhesive kapton™: these rolls are stuck onto the silicon wafer (well separated from each other) and the sample is fixed on top of the rolls. When the RF biasing voltage is applied to the wafer, this air gap acts as a serial condenser, whose capacitance is small compared to the equivalent capacitance of the sheath that is facing the sample. Hence, if the air gap is thick enough it will prevent the dc biasing of the Al_2O_3 sample, while at the same time the wafer holding the sample will be dc-biased and will be etched under regular conditions. The Al_2O_3 sample is thus electrically floating like the reactor walls, and the same deposit grows on the sample and on the reactor walls. After the process, the silicon wafer holding the sample can be transferred *under vacuum* to the XPS analyser through a robotized transfer chamber, and the chemical composition of the deposit formed on the Al_2O_3 sample can be analysed quantitatively. The details of this procedure and the method to analyse the XPS data have been presented in detail in [6].

3. Results and discussion

3.1. Silicon etching in HBr/Cl_2 plasmas without O_2

3.1.1. XPS analyses of the chamber wall coatings. Figure 3 shows the results of the XPS analyses of the Al_2O_3 sample, which represents the reactor walls, before and after its exposure to a silicon etching plasma. Before its exposure to the plasma, the sample consists mainly of Al and O elements (which are grouped for clarity in the figure) with a small carbon contamination that results from the sample exposure to the ambient air before its introduction in the reactor. But figure 3 shows that after sample exposure to the silicon etching plasma for 80 s, the volume probed by XPS (typically the first 10–15 nm in the surface) has almost the same composition as before, if one ignores the appearance of 11% of Cl and 6% of silicon traces. Furthermore, we underline that a longer exposure of the sample to the silicon etching plasma does not result in an increase of the silicon amount detected at the surface of the sample. This indicates that during silicon etching in HBr/Cl_2 plasmas, there is no silicon accumulation on the reactor walls, which basically stay 'clean'.

3.1.2. $SiCl_X$ radical densities. The silicon, SiCl and $SiCl_2$ densities measured by UV absorption during the HBr/Cl_2 silicon etching process are 5×10^{10} cm^{-3}, 1.6×10^{11} cm^{-3} and 3.5×10^{12} cm^{-3}, respectively. The $SiCl_2$ density is thus 20 times larger than the SiCl density, which is itself 70 times larger than the Si atom density. To proceed further, we can

Table 1. Electron impact inelastic reactions, associated rate coefficients (from [15]) and their value (10^{-9} cm^3 s^{-1}) at 3 eV.

Reaction	Rate coefficient (cm^3 s^{-1})	k at $T_e = 3$ eV
$e + SiCl_2 \rightarrow SiCl_2^+ + 2e$	$k_1 = 2.98 \times 10^{-8} \exp(-9.81/T_e)$	1.1
$e + SiCl_2 \rightarrow SiCl^+ + Cl + 2e$	$k_2 = 8.93 \times 10^{-8} \exp(-9.81/T_e)$	3.4
$e + SiCl \rightarrow SiCl^+ + 2e$	$k_3 = 7.54 \times 10^{-8} \exp(-6.79/T_e)$	7.8
$e + SiCl \rightarrow Si^+ + Cl + 2e$	$k_4 = 8.85 \times 10^{-8} \exp(-12.1/T_e)$	1.6
$e + Si \rightarrow Si^+ + 2e$	$k_5 = 7.85 \times 10^{-8} \exp(-7.41/T_e)$	6.6
$e + SiCl_2 \rightarrow SiCl + Cl + e$	$k_6 = 7.27 \times 10^{-9} \exp(-4.99/T_e)$	1.4
$e + SiCl \rightarrow Si + Cl + e$	$k_7 = 7.27 \times 10^{-9} \exp(-3.95/T_e)$	2

also estimate the $SiCl_3 + SiCl_4$ density under these conditions. Since there is no silicon accumulation on the reactor walls, the silicon that leaves the wafer as $SiCl_2$ and $SiCl_4$ volatile species [35] is eliminated from the system only by pumping. The total concentration of silicon containing species in the plasma is then given by

$$\sum_{0 \leqslant X \leqslant 4} [SiCl_X] = \frac{P_{wafer}}{k_{pump}}, \quad (1)$$

where k_{pump} (s^{-1}) is the pumping rate calculated to be about 28 s^{-1} from the total gas flow rate, the pressure and the reactor volume, and P_{wafer} (cm^{-3} s^{-1}) is the production rate of the silicon from the wafer, calculated from the wafer etch rate:

$$P_{wafer} = \frac{10^{-7} E_r S \rho N}{60 m V}, \quad (2)$$

where E_r is the wafer etch rate (180 nm min^{-1} under these conditions), S the wafer area (cm^2), ρ the silicon bulk density (2.33 g cm^{-3}), $N = 6.02 \times 10^{23}$ the Avogadro number, m the atomic silicon mass (g) and V the plasma volume (cm^3). From equation (1), the total concentration of silicon etch products in the plasma should be about 1×10^{13} cm^{-3}. Since the sum of the Si, SiCl and $SiCl_2$ densities measured under these conditions is about 4×10^{12} cm^{-3}, it follows that the sum of the $SiCl_3$ and $SiCl_4$ densities should be about 6×10^{12} cm^{-3}. In conclusion, the $SiCl_2$ and $SiCl_3 + SiCl_4$ densities are comparable, and $SiCl_2$ and $SiCl_4$ that are the predominant etch products from the wafer [35] are also dominant species in the plasma gas phase, and thus the main vectors transporting silicon to the pump. We have shown that under these conditions the Cl_2 was almost fully dissociated [20], and we would expect the same behaviour for the dissociation of $SiCl_2$ and $SiCl_4$ molecules, producing Si atoms. According to the results of Lee *et al* [15], this already suggests that $SiCl_2$ and $SiCl_4$ are also continuously produced from the reactor walls during the process. Clear evidence of this wall production can be obtained by calculating an upper limit for the $SiCl_2$ density in our reactor (called $[SiCl_2]^{max}$), by considering only the production of $SiCl_2$ from the wafer, and by showing that $[SiCl_2]^{max}$ is much lower than the measured density. $[SiCl_2]^{max}$ is calculated by assuming that $SiCl_2$ is the *only* etch product of the silicon wafer (although we have shown above that $SiCl_4$ production is at least as important), and that it is not lost at the reactor walls. The upper limit $SiCl_2$ density is then given by

$$[SiCl_2]^{max} = \frac{P_{wafer}}{[k_1 + k_2 + k_6] n_e + k_{pump}}, \quad (3)$$

where k_1, k_2 and k_6 are the rate coefficients for the electron impact ionization, dissociative ionization and dissociation of $SiCl_2$, respectively (see table 1) and n_e is the electron density. In a similar reactor, Malyshev *et al* [36, 37] have measured $n_e = 5 \times 10^{10}$ cm^{-3} and $T_e = 3$ eV at 5 mTorr pure Cl_2 plasma and 300 W source power. From table 1, at $T_e = 3$ eV the rate coefficients k_1, k_2 and k_6 are 1.1×10^{-9} cm^3 s^{-1}, 3.4×10^{-9} cm^3 s^{-1} and 1.4×10^{-9} cm^3 s^{-1}, respectively, resulting in decay frequencies of 56 s^{-1}, 170 s^{-1} and 70 s^{-1}, respectively.

We then find, under our conditions, an upper limit $SiCl_2$ density $[SiCl_2]^{max} = 1 \times 10^{12}$ cm^{-3}, significantly smaller than the measured density, 3.5×10^{12} cm^{-3}. This shows that there must be another source of $SiCl_2$ than the wafer to explain the measured density, and this source can only be the reactor walls. Hence, the $SiCl_2$ density during silicon etching in Cl_2-based plasmas without O_2 must be calculated by including a $SiCl_2$ radical production term at the reactor walls, at the rate P_{wall}:

$$[SiCl_2] = \frac{P_{wafer} + P_{wall}}{[k_1 + k_2 + k_6] n_e + k_{pump}}. \quad (4)$$

From the above discussion we can conclude that during silicon etching in HBr/Cl_2 the reactor walls stay 'clean', and at the same time they produce $SiCl_2$ and probably also $SiCl_4$ species. Therefore, the silicon etched from the wafer is cycled through the reactor walls and the gas phase, exactly as it has been proposed by Lee *et al* [15] and Kiehlbauch and Graves [38]: the primary etch products of the silicon wafer, $SiCl_2$ and $SiCl_4$, are dissociated and ionized into depositing species (which may only include Si and SiCl radicals and their ions) that stick on the reactor walls. However, the silicon redeposited on the walls is etched by Cl atoms and returns to the plasma as $SiCl_2$ and $SiCl_4$ volatile species, thus, restarting the cycle. This cycle generates high densities of $SiCl_2$ and $SiCl_4$ radicals in the plasma volume even if the gas dissociation rate by electron impacts is high. In other words, a large part of the silicon containing ions and light radicals produced in the plasma volume by electron impact, forms $SiCl_2$ on the reactor walls that return into the plasma volume.

Interestingly, under these conditions, the value of P_{wall} that must be added to the numerator of equation (4) to reach the measured density is about 8.5×10^{14} cm^{-3} s^{-1}, almost three times the $P_{wafer} = 3 \times 10^{14}$ cm^{-3} s^{-1}. It means that the production rate of $SiCl_2$ by the reactor walls is larger than its production rate from the wafer. This is not surprising, since one single $SiCl_2$ molecule produced by the wafer can lead several times to the production of a $SiCl_2$ molecule from the reactor walls following several cycles of dissociation (or ionization), sticking, recycling and so on: the $SiCl_2$ loss rate by pumping

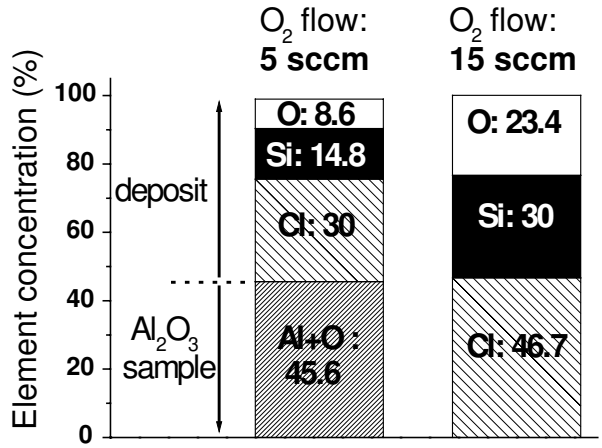

Figure 4. Chemical composition of the ∼10 nm thick layer probed by XPS (Al_2O_3 + deposited layer) after the etching of a blanket silicon wafer in $HBr/Cl_2/O_2$ plasmas with O_2 dilutions of 5 sccm (left) and 15 sccm (right). Other processing conditions as in figure 3.

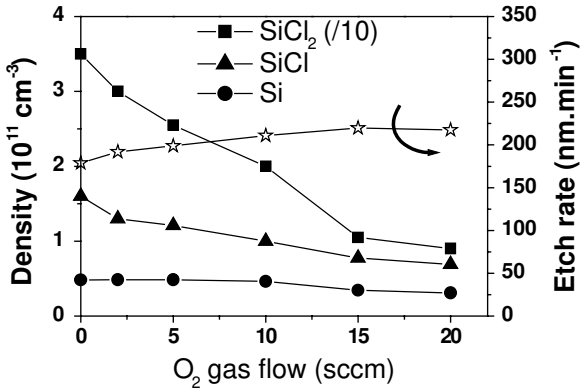

Figure 5. Influence of O_2 gas flow on the absolute concentrations of $SiCl_X$ ($X = 0$–2) etch products, and on the silicon wafer etch rate (ψ). Process conditions as in figure 3 (excepted for O_2 flow) with 300 W RF source power and 90 W RF bias power.

$(28\,s^{-1})$ is small compared to the dissociation and ionization loss rates $(300\,s^{-1})$ both of which lead to the production of lighter radicals and ions that will diffuse rapidly to the reactor walls (typically at a rate of about $1400\,s^{-1}$ for radicals) to produce $SiCl_2$ again.

The fast removal of silicon redeposited on the reactor walls by Cl atoms is not surprising since under our conditions the silicon wafer itself can be etched *without* RF biasing. Finally, we also point out that in addition to the recycling mechanism of silicon described above, the abstraction of Cl atoms adsorbed at the surface by impinging SiCl radicals can also result in the production of $SiCl_2$ species by the reactor walls. This will be discussed in more detail below.

3.2. Influence of O_2 addition on the HBr/Cl_2 etching plasmas

3.2.1. Influence on the reactor walls coatings. Figure 4 shows the XPS analysis of the Al_2O_3 sample, which simulates the reactor wall after its exposure to the HBr/Cl_2 silicon etching plasmas with two different O_2 dilutions (5 sccm and 15 sccm, respectively).

In contrast to figure 3, figure 4 shows that the volume probed by XPS (about 10 nm of the surface layer) now includes two contributions of oxygen (that are separated for clarity in this figure): one from the Al_2O_3 sample, and another one from the silicon oxychloride layer that has been deposited on this sample during the etching process. Therefore, as expected, O_2 addition results in the formation of a chlorine rich silicon oxychloride layer on the reactor walls. With a 5 sccm O_2 flow, the thickness of the deposited layer is estimated to be about 4 nm, according to the mean free path of the photoelectrons in SiOCl material [6]. When the O_2 flow in the process is raised to 15 sccm, figure 4 shows that the layer probed by XPS contains only the silicon oxychloride layer deposited on the sample. This demonstrates that the layer deposited with 15 sccm O_2 is much thicker than the layer deposited with a 5 sccm O_2 flow, since it completely screens the photoelectrons emitted by the Al_2O_3 sample. From this observation we can conclude that the thickness of this layer is greater than 15 nm. However, it appears in figure 4 that the stoichiometry of the layer is not strongly dependent on the O_2 flow used in the process (the layer contains roughly 50% of Cl with both O_2 flows). Hence, increasing the O_2 flow in the etching process results in a dramatic increase of the deposition rate of the silicon oxychloride layer on the reactor walls, but without a significant change in its chemical composition.

3.2.2. Influence on $SiCl_X$ species concentrations. Figure 5 shows the variations of the absolute concentrations of Si, SiCl and $SiCl_2$ radicals in the plasma as a function of the O_2 flow rate in the HBr/Cl_2 gas mixture. Concentrations of silicon etch products in the plasma decrease rapidly with the increasing O_2 flow.

According to equation (4), the decrease of the $SiCl_2$ density with the O_2 flow (figure 5) can be attributed either to a decrease of P_{wafer} or to a decrease of $P_{wall}(n_e, T_e$ and k_{pump} are not expected to vary significantly with small O_2 dilutions, and $SiCl_2$ losses by gas phase chemical reactions with oxygen are negligible at 5 mTorr). However, figure 5 shows that the silicon wafer etch rate increases with the O_2 flow, and we do not expect to have a significant change of the silicon etch products' distribution, since the measured SiO radical density ($<5 \times 10^{10}\,cm^{-3}$) is negligibly small. Therefore, the $SiCl_2$ production rate by the wafer, P_{wafer}, will not change significantly with the O_2 flow rate. It follows (equation (4)) that the decrease of the etch product densities observed in figure 5 when the O_2 flow is increasing can only result from the decrease in the $SiCl_2$ (and $SiCl_4$) production rate by the reactor walls, P_{wall}. This result can be understood according to the schematic of figure 6. As shown in section 3.1, without the addition of O_2, silicon containing species (produced by the dissociation and ionization of $SiCl_2$ and $SiCl_4$, primary etch products of the wafer) diffuse in the plasma volume and stick continuously onto the reactor walls. But at the same time these species are removed from the walls by Cl atoms and return into the plasma volume as $SiCl_2$ and $SiCl_4$. However, in the presence of O atoms, a part of the redeposited silicon is oxidized before being removed from the surface by Cl atoms. The oxidized silicon is, therefore, incorporated into the silicon oxychloride layer deposited on the walls because Cl atoms cannot break a SiO bond [16, 19, 20]. This oxidation mechanism of silicon

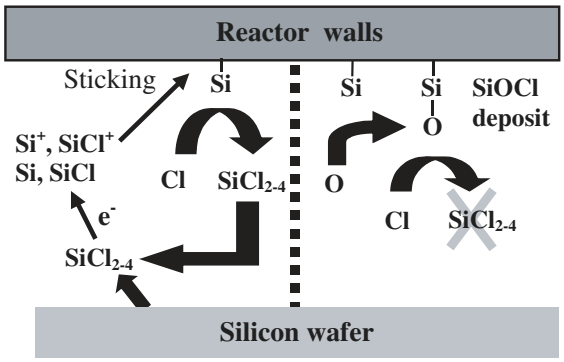

Figure 6. Schematic of the silicon lifecycle and deposition mechanism of the SiO_XCl_y layer on the reactor walls. Left part without O_2: silicon is cycled through the wafer, the reactor walls and the gas phase. $SiCl_2$ and $SiCl_4$ primary etch products of the wafer are dissociated and ionized into depositing species, which are recycled back into the plasma as $SiCl_2$ and $SiCl_4$ after interacting with the walls. On the right with O_2 added: O atoms reduce the silicon lifecycle by fixing it irreversibly on the walls, leading to SiO_XCl_y layer growth and to a decrease in the $SiCl_2$ production rate from the walls.

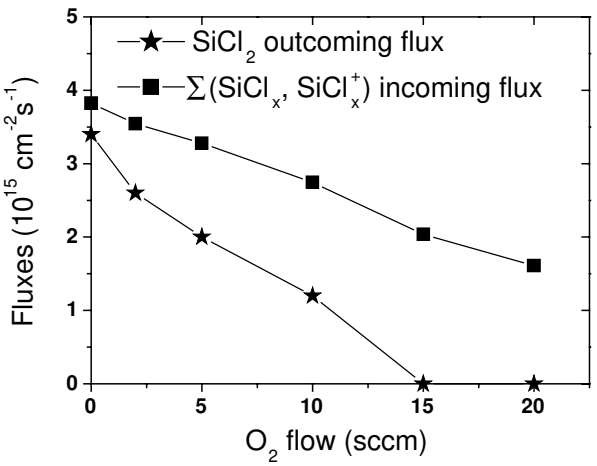

Figure 7. Comparison of the total flux of silicon deposition precursors (Si, SiCl, Si^+ and $SiCl^+$) impinging on the reactor walls with the flux of $SiCl_2$ produced by the reactor walls according to equation (4) by fitting the measured $SiCl_2$ density of figure 5.

trapping on the reactor walls is responsible for the silicon oxychloride film growth. Hence, when the O flow increases, a larger percentage of the silicon containing radicals redeposited on the reactor walls is oxidized and incorporated in the film, instead of being recycled into the plasma, so that the production rate of $SiCl_2$ and $SiCl_4$ from the reactor walls decreases (as observed in figure 5), while at the same time the deposition rate of the silicon oxychloride layer increases (as observed by XPS in figure 4).

According to this schema, the total flux of depositing species (Si, SiCl, Si^+, $SiCl^+$) impinging on the reactor walls must always be significantly larger than the flux of $SiCl_2$ (and $SiCl_4$) produced by the reactor wall surface. Figure 7 compares the flux of $SiCl_2$ produced by the reactor wall with the total flux of silicon precursors impinging on this surface. The latter flux is calculated as the sum of the Si^+ and $SiCl^+$ ion fluxes (from [17]) and the thermal fluxes of Si and SiCl radicals (deduced from their measured density n and the gas temperature T as $(1/4)nv_{\rm th}$, where $v_{\rm th} = (8kT/\pi m)^{1/2}$ is the mean velocity of the radicals). The flux of $SiCl_2$ produced by the reactor wall has been estimated by fitting the measured $SiCl_2$ density with an adjustable value of $P_{\rm wall}$ in equation (4). The flux of $SiCl_2$ produced from the reactor walls is then given by $P_{\rm wall} \times (V/A)$, and can be compared to the total flux of silicon precursors impinging on the surface. In figure 7, the flux of $SiCl_2$ produced by the reactor walls accounts in fact for both $SiCl_2$ and $SiCl_4$, since in our calculation we have assumed that $SiCl_2$ was the only etch product from the wafer. Figure 7 shows that the amount of $SiCl_2$ produced by the reactor walls can be accounted for by the fluxes of silicon precursors incoming to the surface. Without O_2, the flux of $SiCl_2$ produced by the reactor walls represents about 85% of the flux of silicon incident onto the walls, demonstrating that a large percentage of the silicon containing species impinging on the reactor walls is recycled into the plasma as $SiCl_2$ (or $SiCl_4$). This indeed suggests that the surface loss probability of Si, SiCl, Si^+ and $SiCl^+$ on the chamber walls is very large (as will be confirmed hereafter). However, when the O_2 flow increases, the total flux of silicon species impinging on the reactor walls becomes significantly larger than the flux of $SiCl_2$ leaving the reactor walls, because a larger percentage of the incoming silicon is incorporated into the silicon oxychloride layer on the reactor walls instead of being recycled into the plasma as $SiCl_2$. Finally, for O_2 flows above 15 sccm, the production of $SiCl_2$ from the reactor walls becomes negligible, which suggests that all the silicon containing species that get redeposited on the surface are oxidized and definitively incorporated into the film. In this high O_2 flow regime, the deposition rate of the silicon oxychloride layer starts to be limited by the flux of silicon precursors impinging on the surface and by their sticking coefficients (although for lower O_2 flows it is limited by the availability of O atoms only) [13].

3.3. Influence of RF power: estimation of the Si, SiCl and $SiCl_X^+$ sticking probabilities

We have shown that during silicon etching in $HBr/Cl_2/O_2$ plasmas, the removal of silicon redeposited on the reactor walls leads to the production of $SiCl_2$ and $SiCl_4$ volatile molecules from the reactor walls. However, we have not discussed so far the identity of the silicon containing precursors that get redeposited on the reactor walls. As $SiCl_2$ and $SiCl_4$ are discarded, these precursors can include only Si, SiCl and $SiCl_X^+$ ions. As shown in a previous paper [17], high fluxes of Si^+ and $SiCl^+$ ions are impinging on the reactor walls, and furthermore these ions are expected to have a high surface sticking probability due to their about 15 eV kinetic energy (15 eV ions do not need to find a dangling bond to get chemisorbed at the surface). Lee *et al* [15] have suggested that the sticking probability of the ions should be about 0.5. This value is in very good agreement with the value of 0.6 measured by Sakai *et al* [18] for 30 eV $SiCl^+$ ions. Moreover, as shown in table 2, the fluxes of Si-containing ions impinging on the reactor walls are comparable to the thermal flux of Si and SiCl radicals. Therefore, given their high sticking probability, ions are expected to play a significant role in the deposition of silicon on the reactor walls. Furthermore, the ions that do not stick on the reactor walls can be neutralized and returned into

Table 2. Values used in the model as a function of RF source power (W).

RF power	n_e	E_r	Φ_B^{SiCl+}	Φ_B^{Si+}	Φ_{SiCl}	Φ_{Si}
150	2.5	130	0.37	0.02	0.4	0.2
300	5	200	1.25	0.19	1.3	0.8
450	7.5	230	1.75	1.00	1.8	1.9
600	10	250	2.12	1.75	1.5	4

Electron density n_e (10^{10} cm^{-3}), etch rate E_r (nm min^{-1}, measured), $SiCl^+$ and Si^+ ion Bohm flux (10^{15} cm^{-2} s^{-1}, measured) and SiCl and Si thermal fluxes (10^{15} cm^{-2} s^{-1}, deduced from measured densities).

the plasma. By analogy with what was reported in fluorocarbon plasmas [39], this mechanism can be an important channel for the production of Si and SiCl radicals.

The sticking coefficient of the ions on the reactor walls and the surface loss probabilities of Si and SiCl can all be estimated by calculating the Si and SiCl densities with a zero-dimensional model, and by comparing the results to their measured densities. For example, the SiCl density can be calculated by assuming that SiCl is produced both in the gas phase by electron impact dissociation of $SiCl_2$ and at the reactor walls by $SiCl^+$ ion neutralization, with a yield Y (e.g. $1 - Y$ is the ion sticking probability). On the other hand, SiCl is lost from the system by inelastic electron collisions (dissociation and ionization), by pumping, and by reacting at the reactor walls with a probability α that we want to determine.

The SiCl density can then be calculated from the measured density of $SiCl_2$ and from the measured flux of $SiCl^+$ ions impinging on the reactor walls as [40]

$$[SiCl] = \frac{n_e k_6 [SiCl_2] + Y \Phi_B^{SiCl^+} A/V}{(k_3 + k_4 + k_7) n_e + k_{pump} + k_{walls}(\alpha)}, \qquad (5)$$

where k_3, k_4 and k_7 are the electron impact reaction rates for direct ionization, dissociative ionization and dissociation of SiCl, respectively, k_6 is the dissociation rate of $SiCl_2$, Φ_B is the $SiCl^+$ ion Bohm flux and k_{wall} is the loss frequency of SiCl radicals on the reactor walls, given by [41]

$$\frac{1}{k_{walls}(\alpha)} = \frac{\Lambda^2}{D} + \frac{V}{A} \frac{2(2-\alpha)}{v_{th}\alpha}, \qquad (6)$$

where Λ is the characteristic diffusion length, $1/\Lambda^2 = (\pi/L)^2 + (2.405/R)^2$ and D the diffusion coefficient at 5 mTorr. The diffusion coefficients of $SiCl_X$ species in our gas mixture are estimated from the diffusion coefficient of Cl in Cl_2, corrected for the difference in the reduced masses of the two collision pairs [40]. Since the $SiCl_2$ density, Φ_B and the gas temperature are measured in our experiments, and since the electron densities and the reaction rates k are estimated with a reasonably good accuracy from the literature [15, 36], equation (5) can be used to evaluate the SiCl density that is expected from the measured $SiCl_2$ density, Φ_B, Y and α being considered as adjustable parameters. Then, both α and Y can be varied to fit the measured density, which allowed us to get an estimation of their values. This procedure has been applied both to SiCl through equation (5), and also to atomic Si by using a similar procedure [40] (the silicon density is calculated from the measured density of SiCl and from the measured Si^+ ion flux).

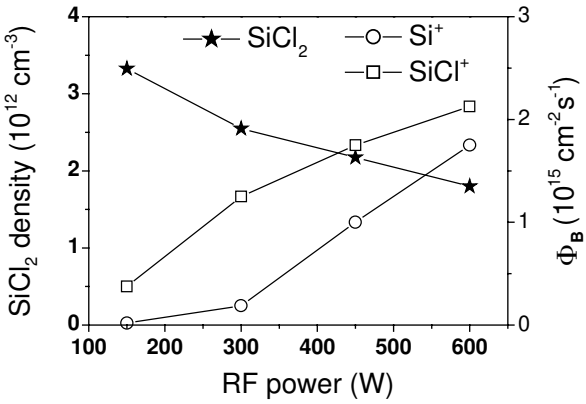

Figure 8. Influence of the RF source power on the $SiCl_2$ density and on the Bohm fluxes of Si^+ and $SiCl^+$ ions (from [17]). Plasma conditions are: HBr (120 sccm)/Cl_2 (60 sccm)/O_2 (5 sccm) gas mixture. RF bias power is 0.3 times the RF source power.

As an example, figure 8 shows the RF power dependent $SiCl_2$ density and Si^+ and $SiCl^+$ ion Bohm fluxes (Φ_B) measured under our conditions, which will be used in the following to calculate the SiCl and Si densities. The RF bias power was varied proportionally to the inductive power so as to maintain a constant energy of the ions impinging on the wafer. We underline that the values of ion fluxes at 150 W RF power suffers from a much larger uncertainty than the other data points since they have been obtained by extrapolating to low RF powers the variations of the ion fluxes with RF power of [17] (the lowest power at which the Si^+ and $SiCl^+$ ion fluxes were measured in [17] in the DPS reactor would correspond to 200 W in the LAM 9400 reactor used in this study).

As the electron density increases with RF power, the dissociation rate of $SiCl_2$ increases leading to a decrease in its density (figure 8). At the same time, the ionization rate (both direct and dissociative) of $SiCl_X$ radicals (with $X \leqslant 2$) increases, leading to an increase in the Si^+ and $SiCl^+$ ion densities. Under these conditions, we assume that n_e increases from 2.5×10^{10} to 1×10^{11} cm^{-3} when the RF inductive power is raised from 150 to 600 W. These values are based on the Langmuir probe and microwave interferometer measurements performed by Malyshev and Donnelly [36] in a pure Cl_2 plasma at 5 mTorr in a reactor similar to the one used in this work. The electron temperature is assumed to be about 3 eV independently of the RF source power.

Figure 9 shows the comparison between the measured and calculated densities of SiCl and Si as a function of the RF inductive power. The result of the calculation is shown for various values of the sticking coefficient α between 0 and 1 and with a value of Y of 0.5 (50% of the ions are assumed to stick on the chamber walls and 50% returns into the plasma as neutral radicals). It appears that a reasonably quantitative fit of the RF power dependence of the radical densities can be achieved with a sticking coefficient α of about 1 for SiCl radicals and 0.2 for Si atoms. We should admit that a large uncertainty exists in these values due to the assumptions inherent to our model (zero-dimensional model assuming homogeneous density of radicals within the plasma volume), and to the uncertainty in the electron density and in the cross sections, and also to the value of Y being used (as discussed later). However, the result

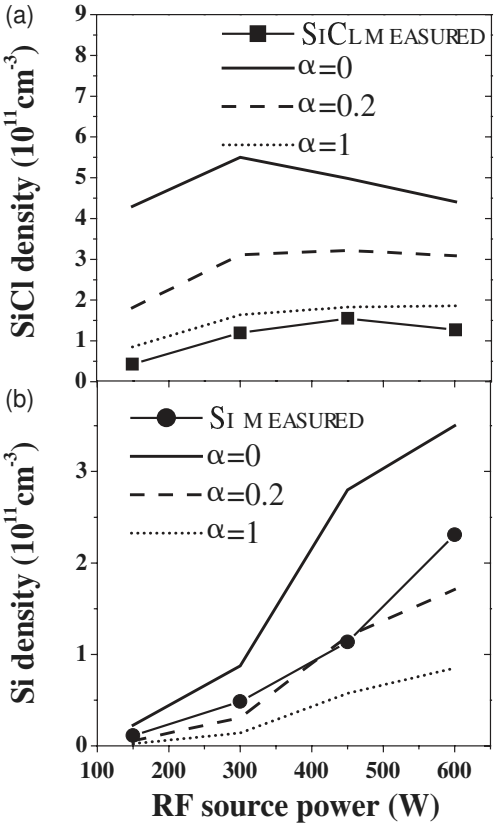

Figure 9. Measured (—■—,—●—) and calculated concentrations of (*a*) SiCl and (*b*) Si radicals as a function of the RF source power for different surface sticking coefficients α (——, $\alpha = 0$, - - - -, $\alpha = 0.2$, · · · · · ·, $\alpha = 1$), with $Y = 0.5$. Same plasma condition as in figure 8.

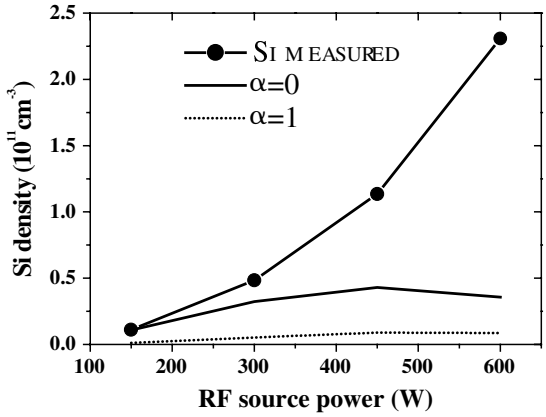

Figure 10. Measured (—●—) and calculated Si atom densities as a function of the RF source power for different surface sticking coefficients α (- - - -, $\alpha = 0$, · · · · · ·, $\alpha = 1$), with $Y = 0$. Same plasma conditions as in figure 8.

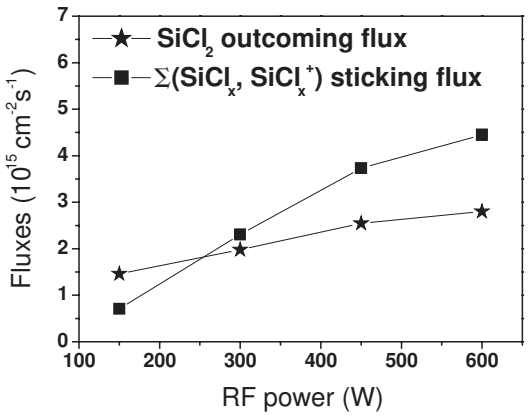

Figure 11. Comparison of the $SiCl_2$ flux produced by the reactor walls with the total flux of silicon deposition precursors (Si, SiCl, Si^+ and $SiCl^+$) reacting with the surface (given by the product of their flux by their surface reaction probability). Same plasma condition as in figure 8.

indicates that the surface loss probability of Si and SiCl on the reactor walls is very high. A value of 0.2 for Si atoms is realistic due to its low vapour pressure. However, the value of $\alpha = 1$ for SiCl cannot be attributed to the chemisorption (sticking) only. But then, in addition to the chemisorption, it is reasonable to assume that abstraction reactions of Cl atoms adsorbed at the surface with incoming SiCl radicals may be another important surface loss channel for SiCl radicals. This reaction will directly lead to the $SiCl_2$ production from the reactor walls without passing through a chemisorbed state of SiCl at the surface.

In the above calculation, we have assumed $Y = 0.5$, following Lee *et al* [15], and the values of α deduced from our fitting procedure clearly depend on this value of Y. However, we underline that a reasonable fit of the RF power dependence of the Si and SiCl densities can only be achieved for values of Y that are close to 0.5 (± 0.2). For example, figure 10 shows the comparison between the measured and calculated density of Si for various values of α but with $Y = 0$. In this case, it appears that the model cannot capture at all (neither quantitatively nor qualitatively) the variations of the silicon atom density with the RF power. It follows that neutralization and reflection of Si^+ and $SiCl^+$ ions on the surfaces exposed to the plasma is an important surface production mechanism of Si and SiCl radicals that cannot be neglected if one wants to model the radical kinetics in the plasma. This is because the fluxes of silicon containing ions impinging on the reactor walls are high.

In conclusion, Si^+ and $SiCl^+$ ions are estimated to stick onto the reactor walls with a probability of about 0.5 (0.6 was measured by Sakai *et al* [18]), while Si atoms stick with a probability of 0.2 and SiCl is lost on the reactor walls with a probability of almost unity. In the case of SiCl, sticking is probably not the only mechanism responsible for its surface loss, but other mechanisms such as abstraction of Cl, which will lead to $SiCl_2$ production from the surface, must also be considered. Since the ion Bohm fluxes and radical thermal fluxes are comparable, we can conclude that during silicon etching both ions and light radicals contribute significantly to the silicon redeposition on the reactor walls.

Finally, we can consider the silicon mass balance at the reactor walls. Figure 11 compares the flux of $SiCl_2$ produced by the reactor walls (corresponding to P_{wall} in equation (4)) with the part of the flux of silicon containing species impinging on the reactor walls and that stay on it, Φ_{in}. This latter is deduced from the sum of the thermal fluxes of Si and SiCl (Φ_{Si} and Φ_{SiCl}) multiplied by their respective sticking

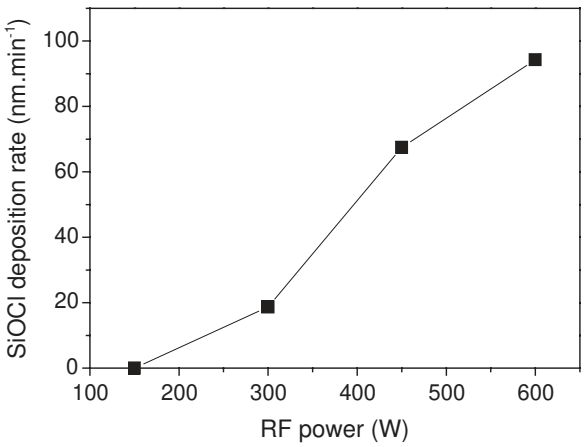

Figure 12. Deposition rate of the silicon oxychloride layer on the reactor walls, calculated from the flux of silicon that reacts with the surface (deduced from figure 11) and by assuming a $SiOCl_2$ layer with a density of $2\,g\,cm^{-3}$. Same plasma conditions as in figure 8.

probability α, and Si^+ and $SiCl^+$ ion Bohm fluxes multiplied by their respective incorporation coefficient $1 - Y$: $\Phi_{in} = \alpha_1\Phi_{Si} + \alpha_2\Phi_{SiCl} + (1 - Y_1)\Phi_B^{Si^+} + (1 - Y_2)\Phi_B^{SiCl^+}$, where the coefficients are taken to be $\alpha_1 = 0.2$, $\alpha_2 = 1$, $(1 - Y_1) = 0.5$ and $(1 - Y_2) = 0.6$ according to the above discussion. Φ_{in} represents the flux of Si actually available to produce $SiCl_2$. Figure 11 shows that for RF powers *above* 150 W, the $SiCl_2$ flux produced from the reactor walls can be accounted for by the total flux of silicon lost on these walls. The deposition rate of the silicon oxychloride layer on the reactor walls is the difference between the flux of silicon sticking on the surface and the flux of silicon leaving it as $SiCl_2$. This result is shown in figure 12, in which we have assumed that the layer composition was $SiOCl_2$ and has a density of $2\,g\,cm^{-3}$. As shown in this figure, the deposition rate of the silicon oxychloride layer rises with RF source power, since the deposition rate is limited by the availability of O atoms and since the flux of O atoms to the reactor wall increases with RF power due to the enhancement of the O_2 dissociation rate. In fact, the deposition rate calculated at 300 W RF power is in very good agreement with the measured [16] deposition rate ($23\,nm\,min^{-1}$), while the deposition rate calculated at 600 W is comparable to the maximum possible deposition rate ($129\,nm\,min^{-1}$) that can be calculated by assuming that 100% of the O_2 molecules injected in the reactor are dissociated in O atoms and that all these O atoms end up in the reactor walls as $SiOCl_2$ film.

However, these deposition rates must be considered with care. In particular, figure 11 shows that at low power (150 W) the model is not suitable to predict the $SiCl_2$ wall produced rate. This disagreement is believed to be partially due to the large uncertainty in the ion fluxes at 150 W (for which we have no experimental data, as mentioned previously). Also, at low RF power, the SiBr and SiBrCl ion densities (neglected here) become comparable to the Si ion density [17]. Furthermore, at low RF source power, the measured Si and SiCl radical densities suffer from a larger uncertainty because their concentrations are small. Finally, the approximations inherent in a zero-dimensional model (no density gradients) can introduce an additional error for all RF powers.

4. Conclusion

Using an industrial silicon etch reactor, we have simultaneously measured the silicon etch rate, the absolute concentration of several silicon etch products and the chemical nature of the layer deposited on the reactor walls during the etching of a 200 mm diameter silicon wafer in $HBr/Cl_2/O_2$ plasmas, with various O_2 dilutions and RF source powers. A detailed analysis of these quantitative data shows that at low oxygen flow rate volatile $SiCl_{2-4}$ species are produced at a high rate from the reactor walls, while this surface constitutes a leakage for Si, SiCl, Si^+ and $SiCl^+$, with probabilities of about 0.2–1 for neutrals and typically about 0.5 for ions. It was shown that the oxidation by O atoms of $SiCl_X$ species chemisorbed on the layer leads to the irreversible incorporation of silicon on the chamber walls by forming a silicon oxychloride film on this surface. Hence, the deposition rate of this layer results from a competition between oxidation by O atoms and the recycling by Cl atoms of the $SiCl_X$ species deposited on the reactor walls. Finally, it was shown that the neutralization and reflection of Si^+ and $SiCl^+$ ions on the reactor walls is a significant source of production of Si and SiCl radicals.

These results are expected to be useful for the improvement and validation of plasma chemistry models, which are widely used for the maturation of plasma reactors and for the feature scale modelling and simulation.

References

[1] Lieberman M A and Lichtenberg A J 1994 *Principle of Plasma Discharges and Material Processing* (New York: Wiley)
[2] ITRS *International Technology Roadmap for Semiconductors* 2002
[3] Guinn K V and Donnelly V M 1993 *J. Appl. Phys.* **75** 2227
[4] Detter X, Palla R, Thomas-Boutherin I, Pargon E, Cunge G, Joubert O and Vallier L 2003 *J. Vac. Sci. Technol.* B **21** 2174
[5] Tuda M, Shintani K and Ootera H 2001 *J. Vac. Sci. Technol.* A **19** 711
[6] Joubert O, Cunge G, Pelissier B, Vallier L, Kogelschatz M and Pargon E 2004 *J. Vac. Sci. Technol.* A **22** 553
[7] Xu S, Sun Z, Qian X, Holland J and Podlesnik D 2000 *J. Vac. Sci. Technol.* B **19** 166
[8] Ullal S J, Godfrey A R, Edelberg E A, Braly L B, Vahedi V and Aydil E S 2002 *J. Vac. Sci. Technol.* A **20** 43
[9] Cunge G, Joubert O and Sadeghi N 2003 *J. Appl. Phys.* **94** 6285
[10] Graves D B and Kushner M J 2003 *J. Vac. Sci. Technol.* A **21** S152
[11] Godfrey A R, Ullal S J, Braly L B, Edelberg E A, Vahedi V and Aydil E S 2001 *Rev. Sci. Instrum.* **72** 3260
[12] Zau G C H and Sawin H H 1992 *J. Electrochem. Soc.* **139** 250
[13] Ullal S J, Singh H, Vahedi V and Aydil E S 2002 *J. Vac. Sci. Technol.* A **20** 499
[14] Cunge G, Kogelschatz M and Sadeghi N 2004 *Plasma Sources Sci. Technol.* **13** 522
[15] Lee C, Graves D B and Lieberman M A 1996 *Plasma Chem. Plasma Process.* **16** 99
[16] Kogelschatz M, Cunge G and Sadeghi N 2004 *J. Vac. Sci. Technol.* A **22** 624
[17] Cunge G, Inglebert R L, Joubert O, Vallier L and Sadeghi N 2002 *J. Vac. Sci. Technol.* B **20** 2137
[18] Sakai T, Sakai A and Okano H 1993 *Japan. J. Appl. Phys.* **32** 3089
[19] Kogelschatz M, Cunge G, Joubert O, Vallier L and Sadeghi N 2004 *Control. Plasma Phys.* **44** 425
[20] Kogelschatz M, Cunge G and Sadeghi N 2004 *J. Phys. D: Appl. Phys.* **37** 1954

[21] Booth J P, Cunge G, Neuilly F and Sadeghi N 1998 *Plasma Sources Sci. Technol.* **7** 423
[22] Augustyniak E, Chew K H, Shohet J L and Woods R C 1999 *J. Appl. Phys.* **85** 87
[23] Wiese W L, Smith M W and Miles B M 1969 *Atomic Transition Probabilities* (US Department of Commerce, National Bureau of Standards, NSRDS-NBS22)
[24] Pearse R W B and Gaydon A G 1965 *The Identification of Molecular Spectra* (London: Chapman and Hall)
[25] Suzuki M, Washida N and Inoue G 1986 *Chem. Phys. Lett.* **131** 24
[26] Becker U, Kerkhoff H, Kwiatkowski M, Schmidt M, Teppner U and Zimmermann P 1980 *Phys. Lett.* A **76** 125
[27] Coutinho L H and Trigueiros A G 2002 *J. Quant. Spectrosc. Radiat. Transfer* **75** 357
[28] Meijer G, Ubachs W, Ter Meulen J J and Dymanus A 1987 *Chem. Phys. Lett.* **139** 603
[29] Engeln R, Mazouffre S, Vankan P, Schram D C and Sadeghi N 2001 *Plasma Sources Sci. Technol.* **10** 595
[30] Sadeghi N 2004 *J. Plasma Fusion Res.* **80** 767
[31] Clarenbach B, Lorenz B, Krämer M and Sadeghi N 2003 *Plasma Sources Sci. Technol.* **12** 345
[32] Velazco J E, Kolts J H and Setser D W 1978 *J. Chem. Phys.* **69** 4357
[33] Braithwaite N S J, Booth J P and Cunge G 1996 *Plasma Sources Sci. Technol.* **5** 677
[34] Cunge G 2003 *56th Gaseous Electronics Conf. (San Francisco)* unpublished
[35] Coburn J W 1994 *J. Vac. Sci. Technol.* B **12** 1384
[36] Malyshev M V and Donnelly V M 2001 *J. Appl. Phys.* **90** 1130
[37] Malyshev M V, Donnelly V M, Kornblit A, Ciampa N A, Colonell J I and Lee J T C 1999 *J. Vac. Sci. Technol.* A **17** 480
[38] Kiehlbauch M W and Graves D B 2003 *J. Vac. Sci. Technol.* A **21** 116
[39] Booth J P, Cunge G, Chabert P and Sadeghi N 1999 *J. Appl. Phys.* **85** 3097
[40] Cunge G, Kogelschatz M and Sadeghi N 2004 *J. Appl. Phys.* **96** 4578
[41] Chantry P J 1987 *J. Appl. Phys.* **62** 1141